熊本大学学術リポジトリ

Bone morphogenetic protein 4 differently promotes distinct VE-cadherin+ precursor stages during the definitive hematopoietic development from embryonic stem cell-derived mesodermal cells

journal or publication title	Experimental hematology
volume	103
page range	40-50.e7
year	2021-11-18
URL	http://hdl.handle.net/2298/00045963

doi: 10.1016/j.exphem.2021.08.008

Bone morphogenetic protein 4 differently promotes distinct VE-cadherin^{+} precursor stages during the definitive hematopoietic development from embryonic stem cell-derived mesodermal cells

Mariko Tsuruda, Saori Morino-Koga, and Minetaro Ogawa*

Department of Cell Differentiation, Institute of Molecular Embryology and Genetics, Kumamoto University, 2-2-1 Honjo, Chuo-ku, Kumamoto 860-0811, Japan

***Corresponding author:** Prof. Minetaro Ogawa, Ph.D., Department of Cell Differentiation, Institute of Molecular Embryology and Genetics, Kumamoto University, 2-2-1 Honjo, Chuo-ku, Kumamoto 860-0811, Japan; Telephone +81 96 373 6591; e-mail, ogawamin@kumamoto-u.ac.jp

Category for the Table of Contents: Stem Cells (embryonic stem cells)

Word count: 3,852 words

The formal publication of this manuscript: DOI: https://doi.org/10.1016/j.exphem.2021.08.008

© 2021. This manuscript version is made available under the CC-BY-NC-ND 4.0 license

https://creativecommons.org/licenses/by-nc-nd/4.0/

Abstract

Definitive hematopoietic cells develop from the fetal liver kinase 1 (Flk1)$^+$ mesodermal cells during the *in vitro* differentiation of mouse embryonic stem cells (ESCs). VE-cadherin$^+$CD41$^-$CD45$^-$ (V$^+$41$^-$45$^-$) hemogenic endothelial cells (HECs) and VE-cadherin$^+$CD41$^+$CD45$^-$ (V$^+$41$^+$45$^-$) cells mediate the definitive hematopoietic development from Flk1$^+$ cells. Bone morphogenetic protein 4 (BMP4) is known to be essential for the formation of mesoderm. However, the role of BMP4 in the differentiation of the VE-cadherin$^+$ definitive hematopoietic precursors from the mesoderm has been elusive. We addressed this issue using a co-aggregation culture of ESC-derived Flk1$^+$ cells with OP9 stromal cells. This culture method induced V$^+$41$^-$45$^-$ cells, V$^+$41$^+$45$^-$ cells, and CD45$^+$ cells from Flk1$^+$ cells. V$^+$41$^+$45$^-$ cells possessed the potentials of erythromyeloid and T-lymphoid differentiation. When Flk1$^+$ cells were cultured in the presence of a high concentration of BMP4, the generation of V$^+$41$^-$45$^-$ cells was enhanced. The increase of V$^+$41$^-$45$^-$ cells led to the subsequent increase of V$^+$41$^+$45$^-$ cells and CD45$^+$ cells. The addition of BMP4 also increased hematopoietic colony-forming cells of various lineages. Furthermore, BMP4 promoted the expansion of V$^+$41$^+$45$^-$ cells independently of the preceding V$^+$41$^-$45$^-$ cell stage. These results suggest that BMP4 has promotive effects on the differentiation of V$^+$41$^-$45$^-$ HECs from Flk1$^+$ mesodermal cells and the subsequent proliferation of V$^+$41$^+$45$^-$ hematopoietic precursors. These findings may provide insights for establishing a culture system to induce definitive hematopoietic stem cells from ESCs.

Keywords: Bone Morphogenetic Protein 4, VE-cadherin, Mouse Embryonic Stem Cells, Mesoderm, Hemogenic Endothelial Cells, Stromal Cells

Introduction

Hematopoietic cells in the mouse embryo develop from fetal liver kinase 1 (Flk1)-expressing lateral mesoderm [1, 2]. The lateral mesoderm generates hemogenic endothelial cells (HECs), from which the definitive hematopoietic cell lineages originate [3]. HECs occur in the vascular endothelium of the extra-embryonic yolk sac and the intra-embryonic paraaortic splanchnopleura at embryonic day (E) 8–9 [3–5]. HECs form the intra-aortic hematopoietic clusters (IAHCs) at E9–10 [6]. Definitive hematopoietic stem cells (HSCs) develop from the IAHCs in the dorsal aorta at E11 [7]. Precursors of HSCs can be categorized into three stages according to the expression of VE-cadherin, CD41, and CD45 [8, 9]. The stages include HECs (VE-cadherin$^+$CD41$^-$CD45$^-$), pre-HSCs type I (VE-cadherin$^+$CD41$^+$CD45$^-$), and pre-HSCs type II (VE-cadherin$^+$CD41$^+$CD45$^+$), listed in developmental order.

Identifying the signaling molecules that regulate the differentiation of HSCs from lateral mesoderm is crucial to achieving *in vitro* generation of HSCs from pluripotent stem cells. Bone morphogenetic protein 4 (BMP4) and its receptor, Bmpr1a/ALK3, are essential for gastrulation and mesoderm formation from the posterior primitive streak [10, 11]. BMP4 promotes the *in vitro* generation of hematopoietic mesoderm from embryonic stem cells (ESCs) [12–15]. BMP4 is continuously required to induce definitive hematopoietic cells from ESCs through Flk1$^+$ blood/endothelial progenitors [16, 17]. However, it has been obscure how BMP4 modulates the developmental processes of definitive hematopoietic cells from the mesoderm.

A co-aggregation culture system with OP9 stromal cells has induced HSCs from embryo-derived HSC precursors [8, 9]. OP9 cells are known initially to provide an efficient microenvironment for inducing *in vitro* differentiation of hematopoietic cells from mouse ESCs [18]. We previously induced definitive hematopoietic progenitors by co-aggregating ESC-derived Flk1$^+$ mesodermal cells with OP9 cells [19]. Using the OP9 co-aggregation culture system, we aimed to examine the impact of BMP4 on the hematopoietic differentiation of Flk1$^+$ cells through VE-cadherin$^+$ hematopoietic precursors.

We found that BMP4 facilitated the differentiation of ESC-derived Flk1$^+$ cells into VE-cadherin$^+$CD41$^-$CD45$^-$ HECs. BMP4 also enhanced the subsequent expansion of VE-cadherin$^+$CD41$^+$CD45$^-$ hematopoietic precursors. Our observation suggests that BMP4 exerts different

functions in distinct VE-cadherin$^+$ precursor stages during the definitive hematopoietic differentiation from mesodermal cells.

Materials and Methods

Cell lines

KTPU8 mouse ESCs [20] were maintained as previously described [21]. OP9 stromal cell line [22] and OP9-DL1 cell line [23], which produces delta-like canonical Notch ligand 1, were maintained in alpha-minimal essential medium (α-MEM) (Gibco™, Thermo Fisher Scientific, Waltham, MA, USA) supplemented with 20% fetal calf serum (FCS) (Japan Bio Serum, Hiroshima, Japan).

Induction of Flk1$^+$ mesodermal cells from ESCs

ESCs (1.3×10^4 cells per culture) were inoculated on an OP9 cell layer prepared in a T25 flask (Nunc™, Thermo Fisher Scientific) and cultured for four days in the induction medium consisting of α-MEM supplemented with 10% FCS (Corning, Woodland, CA, USA) and 50 μM 2-mercaptoethanol (Nacalai Tesque, Kyoto, Japan). Recombinant human/mouse/rat activin A (R&D Systems, Minneapolis, MN, USA) was added at the concentration of 20 ng/ml for the sake of efficient induction of Flk1$^+$ mesodermal cells [19]. Cultured cells were incubated with 0.53 mM EDTA in Hanks' balanced salt solution (Gibco™) and dissociated by gentle pipetting to obtain a single-cell suspension. Cells were stained with phycoerythrin (PE)-conjugated anti-mouse Flk1 monoclonal antibody (mAb) (Avas12, BioLegend, San Diego, CA, USA) followed by labeling with anti-PE microbeads (Miltenyi Biotec, Bergisch Gladbach, German). Flk1$^+$ cells were isolated using a MiniMACS™ separator (Miltenyi Biotec). The purity of Flk1$^+$ cells determined by flow cytometry was routinely more than 95% (98.1±2.3%).

OP9 co-aggregation culture of Flk1$^+$ cells

Cell-aggregates were produced using a modified method based on the previous reports [8, 19]. Flk1$^+$ cells (1×10^5 cells) and OP9 cells (1×10^5 cells) were mixed in a 20 μl induction medium and drawn into a 200 μl OneTouch™ tip (Sorenson, West Salt Lake City, Utah, USA). The tip was sealed with

Parafilm™ (Bemis, Oshkosh, WI, USA) and centrifuged at 1500 rpm for 12 min. The cell-aggregate was dropped onto an MF-Millipore™ 0.8 μm MCE membrane (Merck, Darmstadt, Germany) floating on a 3 ml induction medium and cultured at the liquid-air interface for 1–7 days. Recombinant mouse BMP4 (R&D systems) or recombinant mouse Noggin (BioLegend) was added in the medium with different timing and duration in some experiments. Cultured cell-aggregates were incubated in Collagenase/Disperse™ and dissociated by gentle pipetting to obtain a single-cell suspension. Harvested cells were subjected to flow cytometry analysis, cell sorting, or hematopoietic colony formation assay.

Flow cytometry

The list of the mAbs used in this study is available in the supplemental information. Cells were analyzed using an LE-SP6800Z spectral cell analyzer (SONY, Tokyo, Japan) or sorted using an SH800 cell sorter (SONY).

Hematopoietic cell differentiation assay

Cells harvested from OP9 co-aggregation culture were sorted according to the expression of CD45, CD31, VE-cadherin, and CD41. For differentiation of erythro-myeloid cells, 420 sorted cells were inoculated on an OP9 cell layer prepared in a T25 flask and cultured for seven days in the induction medium supplemented with 20 ng/ml recombinant murine stem cell factor (SCF) (PeproTech, Rocky Hill, NJ, USA), 20 ng/ml recombinant murine interleukin-3 (IL-3) (BioLegend), 2 U/ml recombinant human erythropoietin (EPO), and 20 ng/ml recombinant human granulocyte colony-stimulating factor (G-CSF). EPO and G-CSF were provided by Kyowa Hakko Kirin (Tokyo, Japan). For differentiation of T lymphocytes, 1×10^3 sorted cells were cultured on an OP9-DL1 cell layer for 10–11 days in the induction medium supplemented with 50 ng/ml SCF, 50 ng/ml recombinant murine FMS-like tyrosine kinase 3 ligand (Flt3L) (PeproTech), and 20 ng/ml recombinant murine interleukin-7 (IL-7) (PeproTech). Cells harvested from the erythro-myeloid cultures were analyzed for CD71, TER-119, Gr-1, and CD11b expression by flow cytometry. Cells harvested from the T lymphocyte cultures were analyzed for CD4 and CD8a expression. For cell morphological analyses, cells were spotted onto a glass slide using a

Cytospin 3 (Shandon, Runcorn, UK) and stained using a Hemacolor™ staining kit (Merck). Photomicrographs were obtained using a virtual slide system VS-120 (OLYMPUS, Tokyo, Japan).

Hematopoietic colony assay

Cells dissociated from each cell-aggregate were suspended in a 3 ml of α-MEM supplemented with 1.2% methylcellulose (Muromachi Technos, Tokyo, Japan), 30% FCS (Japan Bio Serum), 1×10^{-4} M 2-mercaptoethanol, 2 mM L-glutamine, 1% bovine serum albumin (Sigma, St. Louis, USA), 20 ng/ml SCF, 20 ng/ml IL-3, 20 ng/ml G-CSF, and 2 U/ml EPO. The cell suspension was plated in a 35-mm petri dish (Falcon™, Corning) at 1 ml per dish and cultured for seven days. Colonies consisting of more than 40 hematopoietic cells were scored.

Statistical analysis

Statistical analyses were performed using GraphPad Prism 6 software (GraphPad Software, La Jolla, CA, USA). Values of $p < 0.05$ were considered statistically significant. Data are presented as mean ± SEM.

Results

OP9 co-aggregation culture induces differentiation of VE-cadherin$^+$CD41$^+$ cells from mesodermal cells

ESCs were co-cultured with OP9 cells for four days to induce Flk1$^+$ mesodermal cells. The Flk1$^+$ cells were isolated by magnetic-activated cell sorting (MACS) (Fig. 1A, B). Re-staining of the purified Flk1$^+$ cells confirmed the absence of VE-cadherin, CD41, and CD45 expression (Fig. 1C). Flk1$^+$ cells were co-aggregated with OP9 cells and cultured at the liquid-air interface on a floating membrane filter for one to seven days (Fig. 1A). Cell-aggregates were dissociated and analyzed by flow cytometry (Fig. 1D). Cell populations were categorized according to the expression of VE-cadherin, CD41, and CD45 (Fig. 1D). Cell number in each cell population per aggregate was calculated from the proportion.

VE-cadherin^{+}CD41^{-}CD45^{-} (V^{+}41^{-}45^{-}) cells increased once on day 1 and decreased to a minimum on day 2 (Fig. 1E). The V^{+}41^{-}45^{-} cells increased again after day 3 and reached a plateau on day 5 (Fig. 1E). Thus, the V^{+}41^{-}45^{-} endothelial cells were generated in two different developmental phases, i.e., an initial temporal phase and a late sustained phase. The number of VE-cadherin^{+}CD41^{lo}CD45^{-} (V^{+}41^{lo}45^{-}) cells showed a similar but mild change as the V^{+}41^{-}45^{-} cells from day 1 to day 3 and had a small peak on day 4 (Fig. 1F). In contrast, VE-cadherin^{+}CD41^{hi}CD45^{-} (V^{+}41^{hi}45^{-}) and VE-cadherin^{-}CD41^{+}CD45^{-} (V^{-}41^{+}45^{-}) cells increased steadily to reach a peak on day 3 and rapidly decreased by day 7 (Fig. 1G, H). VE-cadherin^{+}CD45^{+} (V^{+}45^{+}) cells were always very few and had a small peak on day 3 (Fig. 1I). VE-cadherin^{-}CD45^{+} (V^{-}45^{+}) cells became detectable on day 3 and peaked on day 4 (Fig. 1J).

These results indicate that Flk1^{+} cells sequentially differentiate into V^{+}41^{+}45^{-} cells and CD45^{+} hematopoietic cells in the OP9 co-aggregation culture.

We compared OP9 co-aggregation culture with common OP9 monolayer co-culture (Supplemental Fig. S1A). When Flk1^{+} cells were cultured for four days, the proportion of generated cell populations varied depending on the culture system (Supplemental Fig. S1B–H). Although the total cell recovery was lower than monolayer co-culture, co-aggregation culture generated more V^{+}41^{hi}45^{-}, V^{-}41^{+}45^{-}, V^{+}45^{+}, and V^{-}45^{+} cells (Supplemental Fig. S1I–O). Furthermore, V^{+}41^{-}45^{-} cells in co-aggregation culture did not express Lyve1, resembling endothelial cells in the AGM region, while V^{+}41^{-}45^{-} cells in monolayer co-culture expressed Lyve1 similarly to yolk sac endothelium (Supplemental Fig. S1P, Q).

VE-cadherin^{+}CD31^{+}CD41^{+}CD45^{-} cells have the definitive hematopoietic potentials

We next examined the definitive hematopoietic potentials of VE-cadherin^{+} cell populations isolated from OP9 co-aggregation culture on day 4 (Fig. 2A). CD45^{-}CD31^{+} cells were fractionated according to the expression of VE-cadherin and CD41 into four cell populations, i.e., V^{+}41^{-}, V^{+}41^{lo}, V^{+}41^{hi}, and V^{-}41^{+} cells (Fig. 2B). The sorted cells were cultured on an OP9 cell layer in the presence of SCF, IL-3, EPO, and G-CSF for seven days.

Flow cytometric analyses revealed that more than 75% of the cells derived from the four cell populations were erythroid lineage cells expressing CD71 and TER119 (Fig. 2C). $CD11b^{+}Gr\text{-}1^{-}$ monocytes/macrophages and $CD11b^{+}Gr\text{-}1^{+}$ granulocytes were also detected in all cultures (Fig. 2D). $V^{+}41^{hi}$ cells, which were abundant in co-aggregation culture than monolayer co-culture, generated the highest number of erythrocytes and granulocytes (Fig. 2E, G). $V^{+}41^{lo}$ and $V^{+}41^{hi}$ cells generated a comparable number of monocytes/macrophages (Fig. 2F). The morphological examination confirmed the presence of erythroblasts, enucleated erythrocytes, macrophages, and neutrophils in the cultures of $V^{+}41^{lo}$ and $V^{+}41^{hi}$ cells (Fig. 2H). Although $V^{-}41^{+}$ cells likely represent committed hematopoietic progenitor cells, they produced fewer hematopoietic cells than $V^{+}41^{hi}$ cells (Fig. 2E–G). $V^{+}41^{-}$ cells also produced a small number of erythromyeloid cells (Fig. 2E, F).

We examined the potential of $V^{+}41^{lo}$ and $V^{+}41^{hi}$ cells for T lymphocyte differentiation by culturing with OP9-DL1 cells in the presence of SCF, Flt3L, and IL-7 (Fig. 2A). Both cell populations formed $CD4^{+}CD8^{+}$ T cells (Fig. 2I), although the number of T cells varied among cultures (Fig. 2J).

These results suggest that $V^{+}31^{+}41^{lo}45^{-}$ and $V^{+}31^{+}41^{hi}45^{-}$ cells represent the definitive hematopoietic precursors derived from $Flk1^{+}$ mesodermal cells.

Quantitative PCR analyses of the four-day OP9 co-aggregation culture of $Flk1^{+}$ cells detected a weak expression of *Hoxa9*, a marker of definitive hematopoietic progenitor cells [24–26] (Supplemental Fig. S2A). Adult (*Hbb-bs*) as well as embryonic (*Hbb-y*) hemoglobin was detected (Supplemental Fig. S2A). However, we cannot distinguish whether the definitive hematopoietic differentiation in this model represents the intra-embryonic or extra-embryonic development of the definitive hematopoiesis.

BMP4 enhances the development of hematopoietic progenitors from mesodermal cells

We examined the impact of BMP4 on the hematopoietic differentiation of $Flk1^{+}$ cells through the VE-$cadherin^{+}$ precursors. $Flk1^{+}$ cells were co-aggregated with OP9 cells and cultured in the presence or absence of 100 ng/ml BMP4 (Fig. 3A). Cell number in each population per aggregate was calculated from the proportion determined by flow cytometric analyses (Supplemental Fig. S3). BMP4 significantly increased $V^{+}41^{-}45^{-}$ cells on day 1 (Fig. 3B). However, the increasing effect was not observed on day 2 and day 4, suggesting that the $V^{+}41^{-}45^{-}$ cells that increased on day

1 rapidly differentiated into other cell populations (Fig. 3B). $V^+41^{lo}45^-$ cells showed the same tendency of transient increase on day 1 in response to BMP4 (Fig. 3C). In contrast, BMP4 had no effects on $V^+41^{hi}45^-$ cells on day 1 (Fig. 3D). $V^+41^{hi}45^-$ cells increased on day 2 in the presence of BMP4 and returned to the control level on day 4 (Fig. 3D). Similarly, the increase of $V^-41^+45^-$ cells and V^+45^+ cells was temporally observed on day 2 in the presence of BMP4 (Fig. 3E, F). V^-45^+ hematopoietic cells were not affected by BMP4 until day 2, while BMP4 significantly increased V^-45^+ cells on day 4 (Fig. 3G).

We compared the number of hematopoietic colony-forming cells on day 4. BMP4 dramatically increased colony-forming cells of various hematopoietic lineages (Fig. 3H, I).

These results suggest that BMP4 facilitates the definitive hematopoietic differentiation from $Flk1^+$ mesodermal cells.

BMP4 promotes the formation of VE-cadherin$^+$CD41$^-$CD45$^-$ HECs from mesodermal cells

We next investigated the effect of BMP4 on each cell population undergoing differentiation in the OP9 co-aggregates. BMP4 was added in the OP9 co-aggregation culture of $Flk1^+$ cells on day 1, and cells were analyzed on day 2 (Fig. 4A, Supplemental Fig. S4A). Although $V^+41^{lo}45^-$ cells slightly increased compared to the control culture, we did not observe any significant effects of BMP4 on other cell populations, including $V^+41^{hi}45^-$ cells (Fig. 4A). Therefore, the delayed increase of $V^+41^{hi}45^-$ cells by the two-day treatment with BMP4, shown in Fig. 3D, probably reflected the differentiation of $V^+41^-45^-$ cells that increased on day 1 in the presence of BMP4 (Fig. 3B). These results also suggest that the $V^+41^-45^-$ cells that increase in response to BMP4 likely represent HECs.

BMP4 promotes the expansion of VE-cadherin$^+$CD41^{hi}CD45$^-$ cells

As $V^+41^{hi}45^-$ cells expanded between day 2 and day 3 (Fig. 1G), we next examined the effect of a one-day treatment with BMP4 starting from day 2 (Fig. 4B, Supplemental Fig. S4B). Interestingly, BMP4 increased $V^+41^{hi}45^-$ cells and V^+45^+ cells between day 2 and day 3 (Fig. 4B). In contrast, other cell populations such as $V^+41^-45^-$ cells and $V^+41^{lo}45^-$ cells were not significantly influenced by the BMP4 treatment (Fig. 4B). This result suggests that BMP4 can promote the expansion of $V^+41^{hi}45^-$ cells from

day 2 to day 3 without influencing any earlier cell populations. The increase of V^+45^+ cells, on the other hand, can be due to the increase of $V^+41^{hi}45^-$ cells.

When BMP4 was added from day 3 to day 4, no significant effect was observed in all cell populations examined (Fig. 4C, Supplemental Fig. S4C). While the four-day treatment with BMP4 dramatically increased V^-45^+ hematopoietic cells (Fig. 3G), any of the one-day treatments that started from day 1 to day 3 did not affect V^-45^+ cells (Fig. 4A–C). Therefore, the increase of V^-45^+ cells is suggested to be an indirect effect of the increase of earlier cell populations induced by BMP4.

To directly demonstrate the effect of BMP4 on $V^+41^{hi}45^-$ cells, we isolated $V^+41^{hi}45^-$ cells from the two-day culture of $Flk1^+$ cells and re-aggregated them with fresh OP9 cells (Fig. 5A). As expected, one-day re-aggregation culture in the presence of BMP4 led to the recovery of a higher number of $V^+41^{hi}45^-$ cells than control culture (Fig. 5B, C).

A high concentration of BMP4 is required to increase VE-cadherin$^+$CD41^{hi}CD45$^-$ cells

To examine the concentration dependence of BMP4-induced increase of $V^+41^{hi}45^-$ cells, $Flk1^+$ cells were co-aggregated with OP9 cells and cultured in the presence of 0, 5, 20, 50, or 100 ng/ml BMP4 for two days (Fig. 6A). Treatment of 5–50 ng/ml BMP4 did not influence the number of $V^+41^{hi}45^-$ cells, while 100 ng/ml BMP4 significantly increased $V^+41^{hi}45^-$ cells (Fig. 6B). Therefore, a high concentration of BMP4 was required to increase $V^+41^{hi}45^-$ cells in the OP9 co-aggregation culture.

OP9 cells express BMP4 [27]. *Bmp4* transcripts were detected in the co-aggregation culture at a similar level to E9.5 embryo proper (Supplemental Fig. S2B). We tested whether cell differentiation in the OP9 co-aggregation culture depends on endogenous BMPs. $Flk1^+$ cells were co-aggregated with OP9 cells and cultured in the presence of 400 ng/ml Noggin for one or two days (Fig. 6C). Despite the observation mentioned above that BMP4 increased $V^+41^-45^-$ cells on day 1 (Fig. 3B), Noggin did not influence the $V^+41^-45^-$ cells in the same period (Fig. 6D). Similarly, $V^+41^{hi}45^-$ cells and V^+45^+ cells were not influenced by Noggin on day 2 (Fig. 6E), in contrast to the positive effects of BMP4 (Fig. 3D, F). LDN193189, an ALK2/3 inhibitor, also failed to affect $V^+41^{hi}45^-$ cells and V^+45^+ cells (Supplemental Fig. S5A, C). Other cell populations also remained unchanged in the presence of Noggin (data not shown). In a control experiment, Noggin and LDN193189 inhibited the increase of $V^+41^{hi}45^-$ cells and

V^+45^+ cells induced by exogenous BMP4 (Supplemental Fig. S5A–C). Transcripts of *Noggin* and *Bmper*, both are BMP inhibitors, were detected in the co-aggregation culture at a similar level to the E10.5 AGM region (Supplemental Fig. S2B). These results suggest that endogenous BMPs are not essential for cell differentiation in the OP9 co-aggregation culture of $Flk1^+$ cells.

Cells harvested from the OP9 co-aggregation culture of $Flk1^+$ cells, regardless of the presence or absence of BMP4, failed to engraft bone marrow hematopoiesis of adult recipients (data not shown).

Discussion

This study demonstrated that OP9 co-aggregation culture induced the differentiation of ESC-derived $Flk1^+$ mesodermal cells into $V^+41^+45^-$ cells, which possessed definitive hematopoietic potentials to generate erythro-myeloid and T lymphoid cells. OP9 co-aggregation culture has been shown to induce HSCs from VE-$cadherin^+$ hematopoietic precursors isolated from mouse embryos [9, 28, 29]. Thus, OP9 co-aggregation culture may provide a useful basis for inducing HSCs from ESC-derived mesodermal cells.

We observed two waves of differentiation of $V^+41^-45^-$ endothelial cells from $Flk1^+$ cells, i.e., an early temporal phase and a late sustained phase. The transient nature of the early $V^+41^-45^-$ cells suggests that they rapidly differentiate into their progenies. We hypothesize that the early $V^+41^-45^-$ cells represent the HECs that differentiate into $V^+41^+45^-$ hematopoietic precursors. In contrast, most of the late $V^+41^-45^-$ cells likely represent the common non-hemogenic endothelial cells and contain fewer HECs. BMP4 rapidly and transiently increased the early $V^+41^-45^-$ cells, suggesting that BMP4 promotes the differentiation of $Flk1^+$ cells into HECs. Alternatively, BMP4 may promote the proliferation of the HECs themselves. However, this possibility might be unlikely from the transient nature of the increasing effect of BMP4.

BMP4 also increased $V^+41^{hi}45^-$ hematopoietic precursors when treated in their expanding phase. This effect was not accompanied by an increase of the $V^+41^-45^-$ cells and $V^+41^{lo}45^-$ cells, putative precursor populations of the $V^+41^{hi}45^-$ cells. BMP4 increased the recovery of $V^+41^{hi}45^-$ cells in an

isolation-and-reaggregation culture. These observations suggest that BMP4 directly promotes the expansion of $V^{+}41^{hi}45^{-}$ hematopoietic precursors.

BMP4 has been reported to induce definitive hematopoietic cells from ESCs through $Flk1^{+}$ progenitors [16, 17]. However, the developmental processes that are influenced by BMP4 have not precisely been identified. Our results suggest that BMP4 promotes the differentiation of $V^{+}41^{-}45^{-}$ HECs from $Flk1^{+}$ cells and the proliferation of $V^{+}41^{hi}45^{-}$ cells. To the best of our knowledge, this is the first study to demonstrate the activity of BMP4 on the distinct VE-cadherin^{+} definitive hematopoietic precursors derived from mesodermal cells.

A high concentration of BMP4 was required to exert an increasing effect on $V^{+}41^{hi}45^{-}$ cells. Aggregating the OP9 cells has been shown to enhance their expression of BMP binding endothelial regulator (BMPER), which antagonizes the BMP activity [30]. We confirmed the presence of *Bmper* transcripts in our OP9 co-aggregation culture. Therefore, it can be assumed that the addition of a low concentration of BMP4 was not effective due to the presence of a large amount of BMP antagonists such as BMPER in this culture system. As an influence of serum cannot be excluded too, a serum-free condition needs to be established to refine the culture system further.

The differentiation of VE-cadherin^{+} pre-HSCs from HECs occurs in the ventral domain of the dorsal aorta (AoV) of E9.5–10.5 mouse embryos. Mesenchymal cells underneath the endothelium of AoV at this embryonic stage express BMP4 [31, 32]. Phosphorylation of Smad1/5/8, which indicates the activation of the BMP signaling pathway, has been detected in the endothelium of AoV and the basal portion of IAHCs [30, 31]. Endothelial cells and IAHCs of E10.5–11 AoV have been shown to express a GFP reporter under the control of the BMP responsive element [33]. The E11 GFP^{+} cells were capable of repopulating bone marrow hematopoiesis of adult recipients. Considering the lifetime of GFP proteins, it is reasonable to assume that the VE-cadherin^{+} precursors that give rise to HSCs receive BMP signals at E9.5–11. Although BMP4 has been proposed to inhibit the differentiation of pre-HSCs II into HSCs [30, 31, 33], BMP4 may drive the HSC development by influencing the VE-cadherin^{+} precursors earlier than pre-HSCs II.

Similarly, BMP4 may modulate the potential of ESC-derived VE-cadherin^{+} precursors toward HSC development in the OP9 co-aggregation culture, even though BMP4 is not essential for the generation of the precursors. Further research is needed to establish whether BMP4 can facilitate the induction of transplantable HSCs from ESCs.

In conclusion, our study elucidated separate functions of BMP4 in the development of definitive hematopoietic precursors from ESC-derived mesodermal cells. The findings should make an important contribution to establishing a culture system that allows the derivation of functional HSCs from pluripotent stem cells.

Data Availability Statement

The datasets generated and analyzed during the current study are available from the corresponding author on reasonable request.

Author contributions

Mariko Tsuruda: Conception and design, collection and assembly of data, data analysis and interpretation, manuscript writing, final approval of the manuscript

Saori Koga-Morino: Conception and design, data analysis and interpretation, final approval of the manuscript

Minetaro Ogawa: Conception and design, financial support, data analysis and interpretation, manuscript writing, final approval of the manuscript

Competing interests

The authors have no potential conflicts of interest to declare.

Acknowledgments

We would like to thank all the members of the Department of Cell Differentiation, Institute of Molecular Embryology and Genetics, Kumamoto University. We also thank the Liaison Laboratory Research Promotion Center of our institute for their technical assistance. This work was supported by JSPS KAKENHI Grant Numbers 15K07081 (MO) and 18K06262 (MO).

References

1. Kataoka H, Takakura N, Nishikawa S, et al. Expressions of PDGF receptor alpha, c-Kit and Flk1 genes clustering in mouse chromosome 5 define distinct subsets of nascent mesodermal cells. DEV. GROWTH DIFFER. 1997;39(6):729–740.
2. Motoike T, Markham DW, Rossant J, et al. Evidence for novel fate of Flk1+ progenitor: contribution to muscle lineage. GENESIS 2003;35(3):153–159.
3. Dzierzak E, Bigas A. Blood development: hematopoietic stem cell dependence and independence. CELL STEM CELL 2018;22(5):639–651.
4. Swiers G, Baumann C, O'Rourke J, et al. Early dynamic fate changes in haemogenic endothelium characterized at the single-cell level. NAT. COMMUN. 2013;4:2924.
5. Yokomizo T, Ogawa M, Osato M, et al. Requirement of Runx1/AML1/PEBP2alphaB for the generation of haematopoietic cells from endothelial cells. GENES CELLS 2001;6(1):13–23.
6. Yokomizo T, Dzierzak E. Three-dimensional cartography of hematopoietic clusters in the vasculature of whole mouse embryos. DEVELOPMENT 2010;137(21):3651–3661.
7. de Bruijn MFTR, Ma X, Robin C, et al. Hematopoietic stem cells localize to the endothelial cell layer in the midgestation mouse aorta. IMMUNITY 2002;16(5):673–683.
8. Rybtsov S, Batsivari A, Bilotkach K, et al. Tracing the origin of the HSC hierarchy reveals an SCF-dependent, IL-3-independent CD43(-) embryonic precursor. STEM CELL REP. 2014;3(3):489–501.
9. Rybtsov S, Sobiesiak M, Taoudi S, et al. Hierarchical organization and early hematopoietic

specification of the developing HSC lineage in the AGM region. J. EXP. MED. 2011;208(6):1305–1315.

10. Winnier G, Blessing M, Labosky PA, et al. Bone morphogenetic protein-4 is required for mesoderm formation and patterning in the mouse. GENES DEV. 1995;9(17):2105–2116.
11. Mishina Y, Suzuki A, Ueno N, et al. Bmpr encodes a type I bone morphogenetic protein receptor that is essential for gastrulation during mouse embryogenesis. GENES DEV. 1995;9(24):3027–3037.
12. Park C, Afrikanova I, Chung YS, et al. A hierarchical order of factors in the generation of FLK1- and SCL-expressing hematopoietic and endothelial progenitors from embryonic stem cells. DEVELOPMENT 2004;131(11):2749–2762.
13. Kattman SJ, Witty AD, Gagliardi M, et al. Stage-specific optimization of activin/nodal and BMP signaling promotes cardiac differentiation of mouse and human pluripotent stem cell lines. CELL STEM CELL 2011;8(2):228–240.
14. Ng ES, Azzola L, Sourris K, et al. The primitive streak gene Mixl1 is required for efficient haematopoiesis and BMP4-induced ventral mesoderm patterning in differentiating ES cells. DEVELOPMENT 2005;132(5):873–884.
15. Pearson S, Cuvertino S, Fleury M, et al. In vivo repopulating activity emerges at the onset of hematopoietic specification during embryonic stem cell differentiation. STEM CELL REP. 2015;4(3):431–444.
16. Lengerke C, Schmitt S, Bowman TV, et al. BMP and Wnt specify hematopoietic fate by activation of the Cdx-Hox pathway. CELL STEM CELL 2008;2(1):72–82.
17. Chiang P-M, Wong PC. Differentiation of an embryonic stem cell to hemogenic endothelium by defined factors: essential role of bone morphogenetic protein 4. DEVELOPMENT 2011;138(13):2833–2843.
18. Nakano T, Kodama H, Honjo T. Generation of lymphohematopoietic cells from embryonic stem cells in culture. SCIENCE 1994;265(5175):1098–1101.
19. Hirota S, Ogawa M. Activin A in combination with OP9 cells facilitates development of Flk-1(+) PDGFRα(-) and Flk-1(+) PDGFRα(+) hematopoietic mesodermal cells from murine embryonic

stem cells. BIOCHEM. BIOPHYS. RES. COMMUN. 2015;467(3):583–588.

20. Nakahara M, Tateyama H, Araki M, et al. Gene-trap mutagenesis using Mol/MSM-1 embryonic stem cells from MSM/Ms mice. MAMM. GENOME 2013;24(5-6):228–239.

21. Park S-H, Sakamoto H, Tsuji-Tamura K, et al. Foxo1 is essential for in vitro vascular formation from embryonic stem cells. BIOCHEM. BIOPHYS. RES. COMMUN. 2009;390(3):861–866.

22. Kodama H, Nose M, Niida S, et al. Involvement of the c-kit receptor in the adhesion of hematopoietic stem cells to stromal cells. EXP. HEMATOL. 1994;22(10):979–984.

23. Hashimoto K, Fujimoto T, Shimoda Y, et al. Distinct hemogenic potential of endothelial cells and CD41+ cells in mouse embryos. DEV. GROWTH DIFFER. 2007;49(4):287–300.

24. Lawrence HJ, Helgason CD, Sauvageau G, et al. Mice bearing a targeted interruption of the homeobox gene HOXA9 have defects in myeloid, erythroid, and lymphoid hematopoiesis. BLOOD 1997;89(6):1922–1930.

25. Pineault N, Helgason CD, Lawrence HJ, et al. Differential expression of Hox, Meis1, and Pbx1 genes in primitive cells throughout murine hematopoietic ontogeny. EXP. HEMATOL. 2002;30(1):49–57.

26. McKinney-Freeman S, Cahan P, Li H, et al. The transcriptional landscape of hematopoietic stem cell ontogeny. CELL STEM CELL 2012;11(5):701–714.

27. Shiraki N, Yoshida T, Araki K, et al. Guided differentiation of embryonic stem cells into Pdx1-expressing regional-specific definitive endoderm. STEM CELLS 2008;26(4):874–885.

28. Sheridan JM, Taoudi S, Medvinsky A, et al. A novel method for the generation of reaggregated organotypic cultures that permits juxtaposition of defined cell populations. GENESIS 2009;47(5):346–351.

29. Taoudi S, Gonneau C, Moore K, et al. Extensive hematopoietic stem cell generation in the AGM region via maturation of VE-cadherin+CD45+ pre-definitive HSCs. CELL STEM CELL 2008;3(1):99–108.

30. McGarvey AC, Rybtsov S, Souilhol C, et al. A molecular roadmap of the AGM region reveals BMPER as a novel regulator of HSC maturation. J. EXP. MED. 2017;214(12):3731–3751.

31. Souilhol C, Gonneau C, Lendinez JG, et al. Inductive interactions mediated by interplay of

asymmetric signalling underlie development of adult haematopoietic stem cells. NAT. COMMUN. 2016;7:10784.

32. Pimanda JE, Donaldson IJ, de Bruijn MFTR, et al. The SCL transcriptional network and BMP signaling pathway interact to regulate RUNX1 activity. PROC. NATL. ACAD. SCI. USA 2007;104(3):840–845.

33. Crisan M, Kartalaei PS, Vink CS, et al. BMP signalling differentially regulates distinct haematopoietic stem cell types. NAT. COMMUN. 2015;6:8040.

Figure Legends

Figure 1. VE-cadherin^{+}CD41^{+}CD45^{-} cells are transiently generated in OP9 co-aggregation culture

(A) Schematic diagram of ESC differentiation culture. ESCs were cultured on an OP9 cell layer for four days. Flk1^{+} mesodermal cells were isolated by MACS and aggregated with OP9 cells. Cell-aggregates were cultured on a membrane filter for 1–7 days and analyzed by flow cytometry. (B) Representative profiles of Flk1 expression on unsorted and sorted cells on day 0. Numbers indicate the percentage of cells in the rectangular regions. (C) Representative profiles of VE-cadherin, CD41, and CD45 expression on sorted Flk1^{+} cells. Flk1^{+} cells isolated by MACS were re-stained and analyzed by flow cytometry. Numbers indicate the percentage of cells in the rectangular regions. Three independent experiments were performed. (D) Representative profiles of VE-cadherin, CD41, and CD45 expression on cultured cells. Flk1^{+} cells were co-aggregated with OP9 cells and cultured for 1–7 days, and analyzed for VE-cadherin, CD41, and CD45 expression by flow cytometry. Upper panels show the profiles of ungated living cells. Lower panels show the profiles of CD45^{-} cells. Numbers indicate the percentage of cells in the rectangular regions. Three independent experiments were performed. The nomenclature of cell populations is depicted in the rightmost panels. (E–J) Time course of the number of VE-cadherin^{+}CD41^{-}CD45^{-} (V^{+}41^{-}45^{-}) cells (E), VE-cadherin^{+}CD41^{lo}CD45^{-} (V^{+}41^{lo}45^{-}) cells (F), VE-cadherin^{+}CD41^{hi}CD45^{-} (V^{+}41^{hi}45^{-}) cells (G), VE-cadherin^{-}CD41^{+}CD45^{-} (V^{-}41^{+}45^{-}) cells (H), VE-cadherin^{+}CD45^{+} (V^{+}45^{+}) cells (I), and VE-cadherin^{-}CD45^{+} (V^{-}45^{+}) cells (J) per aggregate. Three independent experiments were performed.

Figure 2. VE-cadherin$^+$CD31$^+$CD41$^+$CD45$^-$ cells have the definitive hematopoietic potential

(A) Schematic diagram of hematopoietic differentiation assay. ESC-derived Flk1$^+$ cells and OP9 cells were co-aggregated and cultured for four days. CD45$^-$CD31$^+$ cells were fractionated and sorted into V$^+$41$^-$, V$^+$41^{lo}, V$^+$41^{hi}, and V$^-$41$^+$ cells by FACS. To induce erythro-myeloid cells, sorted cells (420 cells per culture) were re-cultured on an OP9 cell layer in the presence of SCF, IL-3, EPO, and G-CSF for seven days. To induce T lymphoid cells, V$^+$41^{lo} or V$^+$41^{hi} cells (one thousand cells per culture) were re-cultured on an OP9-DL1 cell layer in the presence of SCF, Flt3L, and IL-7 for 10–11 days. Cultured cells were analyzed by flow cytometry and stained with Hemacolor. (B) The sorting strategy of cell populations. Representative profiles from five independent experiments are shown. Numbers indicate the percentage of cells in the rectangular regions. (C, D) Representative profiles of the expression of CD71 and Ter119 (C); and CD11b and Gr-1 (D) on the cells cultured in the erythro-myeloid condition. Numbers indicate the percentage of cells in the rectangular regions. Three independent experiments were performed. (E–G) The number of CD71$^+$ and/or Ter119$^+$ erythroid cells (E), CD11b$^+$Gr-1$^-$ monocytes/macrophages (F) and CD11b$^+$Gr-1$^+$ granulocytes (G) per flask. n=6 from three independent experiments. *$p < 0.05$, **$p < 0.01$, ***$p < 0.001$ in Tukey's multiple comparison test. (H) Morphology of hematopoietic cells generated in V$^+$41^{lo} and V$^+$41^{hi} cell cultures. Cytospots were stained with Hemacolor, and photomicrographs were taken by using a VS-120 virtual slide system. Arrows point to the indicated lineage cells. The scale bars indicate 20 μm. (I) Representative profiles of CD4 and CD8 expression on the cells cultured in the T lymphoid condition. Numbers indicate the percentage of cells in each quadrant. Three independent experiments were performed. (J) The number of CD4$^+$CD8$^+$ T cells per flask. n=5 from three independent experiments.

Figure 3. BMP4 increases VE-cadherin$^+$CD41$^-$CD45$^-$ cells, VE-cadherin$^+$CD41^{hi}CD45$^-$ cells, and CD45$^+$ cells in OP9 co-aggregation culture

(A) Experimental design. ESC-derived Flk1$^+$ cells and OP9 cells were co-aggregated and cultured in the presence or absence of BMP4 (100ng/ml) for one, two, or four days. Cultured cells were analyzed for VE-cadherin, CD41, and CD45 expression by flow cytometry. (B–G) The number of VE-

cadherin^{+}CD41^{-}CD45^{-} ($V^{+}41^{-}45^{-}$) cells (B), VE-cadherin^{+}CD41^{lo}CD45^{-} ($V^{+}41^{lo}45^{-}$) cells (C), VE-cadherin^{+}CD41^{hi}CD45^{-} ($V^{+}41^{hi}45^{-}$) cells (D), VE-cadherin^{-}CD41^{+}CD45^{-} ($V^{-}41^{+}45^{-}$) cells (E), VE-cadherin^{+}CD45^{+} ($V^{+}45^{+}$) cells (F), and VE-cadherin^{-}CD45^{+} ($V^{-}45^{+}$) cells (G) per aggregate in the presence (solid lines) or absence (dashed lines) of BMP4. n=4 from four independent experiments (one and two days) or n=5 from five independent experiments (four days). *$p < 0.05$, **$p < 0.01$, ***$p < 0.001$ in paired t-test at each time point. (H) The number of hematopoietic cell colonies. Flk1^{+} cells and OP9 cells were co-aggregated and cultured in the presence or absence of 100 ng/ml BMP4 for four days. One-third of cells dissociated from each aggregate was plated in a dish for hematopoietic colony formation assay (see Materials and Methods). n=8 (Ctrl) and n=10 (BMP4) from three independent experiments. ****$p < 0.0001$ in Student's t-test. (I) Types of hematopoietic cell colonies. BFU-E, burst-forming unit-erythroid; E, erythrocytes; M, monocytes/macrophages; G, granulocytes.

Figure 4. Short-term treatment of BMP4 increases VE-cadherin^{+}CD41^{hi}CD45^{-} cells

(A-C) BMP4 (100 ng/ml) was added in the OP9 co-aggregation culture of Flk1^{+} cells on day 1 (A), day 2 (B), or day 3 (C). After a one-day treatment of BMP4, cells were analyzed for VE-cadherin, CD41, and CD45 expression by flow cytometry. The number of VE-cadherin^{+}CD41^{-}CD45^{-} ($V^{+}41^{-}45^{-}$) cells, VE-cadherin^{+}CD41^{lo}CD45^{-} ($V^{+}41^{lo}45^{-}$) cells, VE-cadherin^{+}CD41^{hi}CD45^{-} ($V^{+}41^{hi}45^{-}$) cells, VE-cadherin^{-}CD41^{+}CD45^{-} ($V^{-}41^{+}45^{-}$) cells, VE-cadherin^{+}CD45^{+} ($V^{+}45^{+}$) cells, and VE-cadherin^{-}CD45^{+} ($V^{-}45^{+}$) cells per aggregate in the presence (hatched bars) or absence (white bars) of BMP4 was determined. n=3 from three independent experiments. *$p < 0.05$ in paired t-test.

Figure 5. BMP4 promotes the expansion of VE-cadherin^{+}CD41^{hi}CD45^{-} cells

(A) Experimental design. VE-cadherin^{+}CD41^{hi}CD45^{-} cells were sorted from OP9 co-aggregation culture of Flk1^{+} cells on day 2. Sorted cells (1×10^{4} cells) were re-aggregated with fresh OP9 cells (1×10^{5} cells) and cultured in the presence or absence of 100 ng/ml BMP4 for one day. Cultured cell-aggregates were dissociated using Collagenase/Disperse™ and analyzed by flow cytometry. (B) Representative profiles of VE-cadherin, CD41, and CD45 expression on cultured cells. Upper panels show the profiles of ungated living cells. Lower panels show the profiles of CD45^{-} cells. Numbers indicate the percentage

of cells in the rectangular regions. (C) The number of VE-cadherin^{+}CD41^{hi}CD45^{-} (V^{+}41^{hi}45^{-}) cells per aggregate. n=3 from three independent experiments. *$p < 0.05$ in paired t-test.

Figure 6. A high concentration of BMP4 is required for the increase of VE-cadherin^{+}CD41^{hi}CD45^{-} cells

(A) Experimental design. ESC-derived Flk1^{+} cells and OP9 cells were co-aggregated and cultured for two days in the presence of various concentrations of BMP4. Cultured cells were analyzed for VE-cadherin, CD41, and CD45 expression by flow cytometry. (B) The number of VE-cadherin^{+}CD41^{hi}CD45^{-} (V^{+}41^{hi}45^{-}) cells per aggregate. n=5 from five independent experiments. **$p < 0.01$ in Dunnett's multiple comparison test. (C) Experimental design. Flk1^{+} cells and OP9 cells were co-aggregated and cultured in the presence or absence of Noggin (400 ng/ml) for one or two days. Cultured cells were analyzed for VE-cadherin, CD41, and CD45 expression by flow cytometry. (D, E) The number of VE-cadherin^{+}CD41^{-}CD45^{-} (V^{+}41^{-}45^{-}) cells on day 1 (D); and VE-cadherin^{+}CD41^{hi}CD45^{-} (V^{+}41^{hi}45^{-}) and VE-cadherin^{+}CD45^{+} (V^{+}45^{+}) cells on day 2 (E) in the presence (black bars) or absence (white bars) of Noggin. n=3 from three independent experiments. P values in Student's t-test are shown.

Figure 1

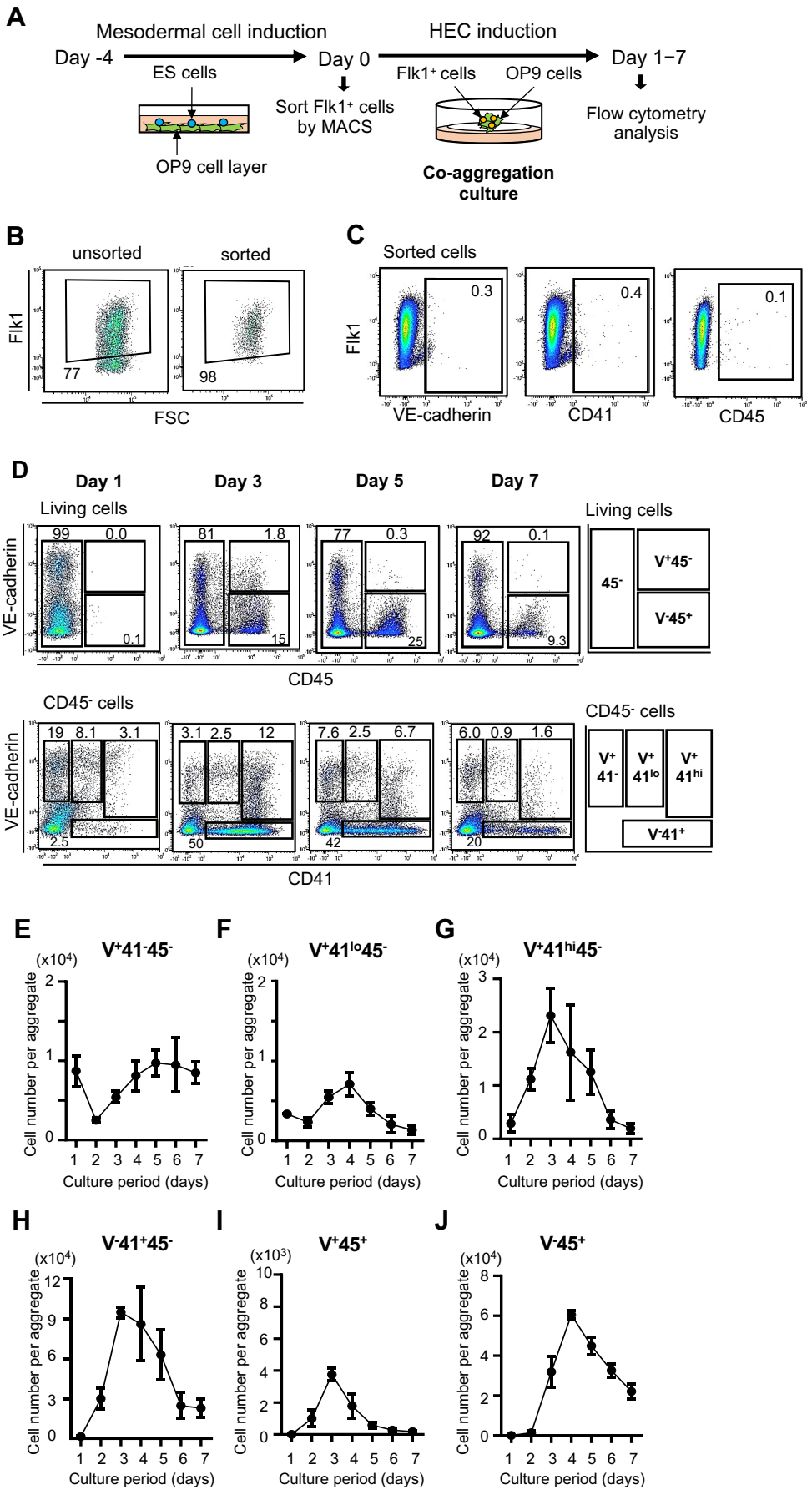
A
Mesodermal cell induction
Day -4
ES cells
OP9 cell layer
Day 0
Sort Flk1+ cells by MACS
HEC induction
Flk1+ cells
OP9 cells
Co-aggregation culture
Day 1−7
Flow cytometry analysis
B
unsorted
sorted
Flk1
77
98
FSC
C
Sorted cells
Flk1
0.3
0.4
0.1
VE-cadherin
CD41
CD45
D
Day 1
Day 3
Day 5
Day 7
Living cells
VE-cadherin
99
0.0
0.1
81
1.8
15
77
0.3
25
92
0.1
9.3
CD45
45-
V+45-
V-45+
CD45- cells
19
8.1
3.1
2.5
3.1
2.5
12
50
7.6
2.5
6.7
42
6.0
0.9
1.6
20
CD41
V+ 41-
V+ 41lo
V+ 41hi
V-41+
E
V+41-45-
F
V+41lo45-
G
V+41hi45-
H
V-41+45-
I
V+45+
J
V-45+
(x10⁴)
(x10³)
Cell number per aggregate
Culture period (days)

Figure 2

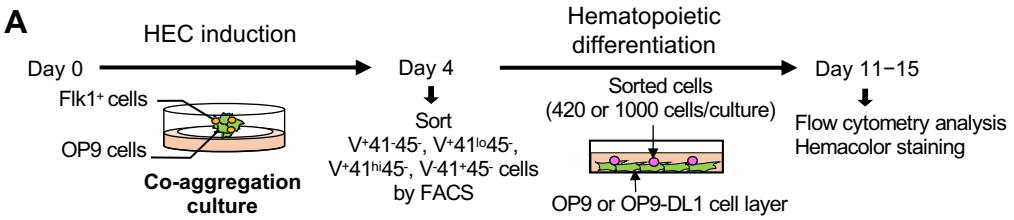
A
HEC induction
Day 0
Flk1+ cells
OP9 cells
Co-aggregation culture
Day 4
Sort
V+41-45-, V+41lo45-, V+41hi45-, V-41+45- cells by FACS
Hematopoietic differentiation
Sorted cells
(420 or 1000 cells/culture)
OP9 or OP9-DL1 cell layer
Day 11−15
Flow cytometry analysis
Hemacolor staining

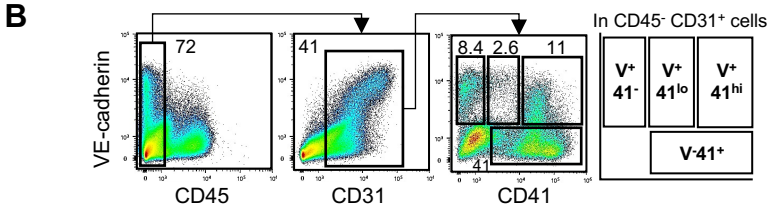
B
VE-cadherin
CD45
CD31
CD41
72
41
8.4
2.6
11
41
In CD45- CD31+ cells
V+ 41-
V+ 41lo
V+ 41hi
V-41+

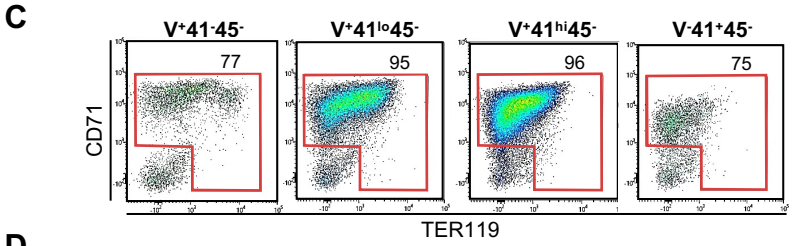
C
V+41-45-
V+41lo45-
V+41hi45-
V-41+45-
77
95
96
75
CD71
TER119

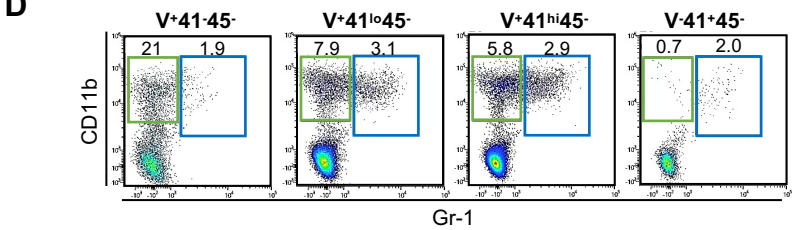
D
V+41-45-
V+41lo45-
V+41hi45-
V-41+45-
21
1.9
7.9
3.1
5.8
2.9
0.7
2.0
CD11b
Gr-1

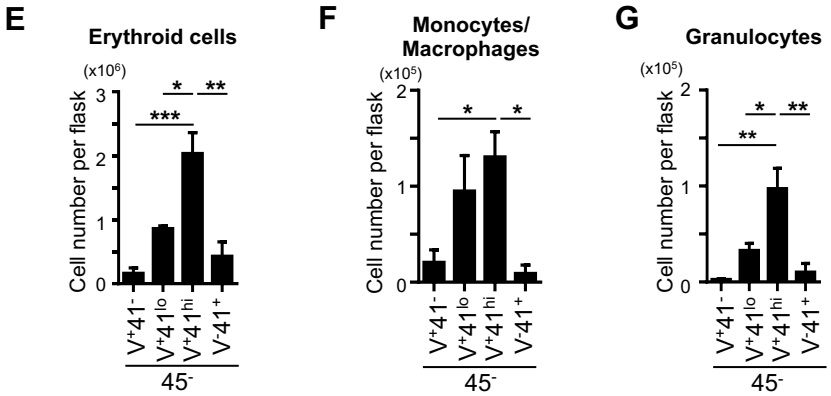
E
Erythroid cells
(x10^6)
Cell number per flask
F
Monocytes/ Macrophages
(x10^5)
G
Granulocytes
(x10^5)
V+41-
V+41lo
V+41hi
V-41+
45-

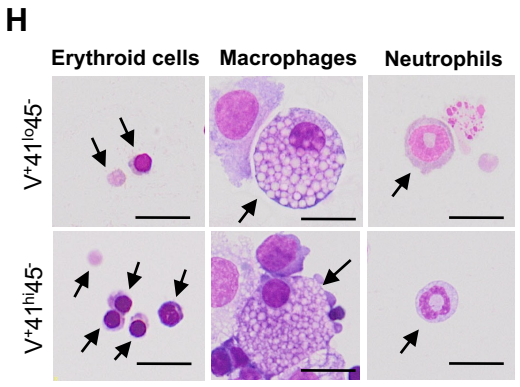
H
Erythroid cells
Macrophages
Neutrophils
V+41lo45-
V+41hi45-

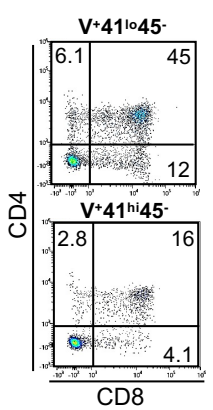
I
V+41lo45-
6.1
45
12
V+41hi45-
2.8
16
4.1
CD4
CD8

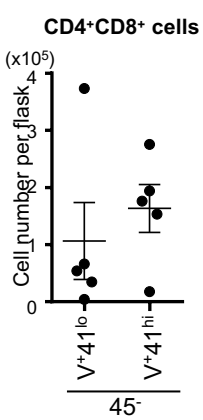
J
CD4+CD8+ cells
(x10^5)
Cell number per flask
V+41lo
V+41hi
45-

Figure 3

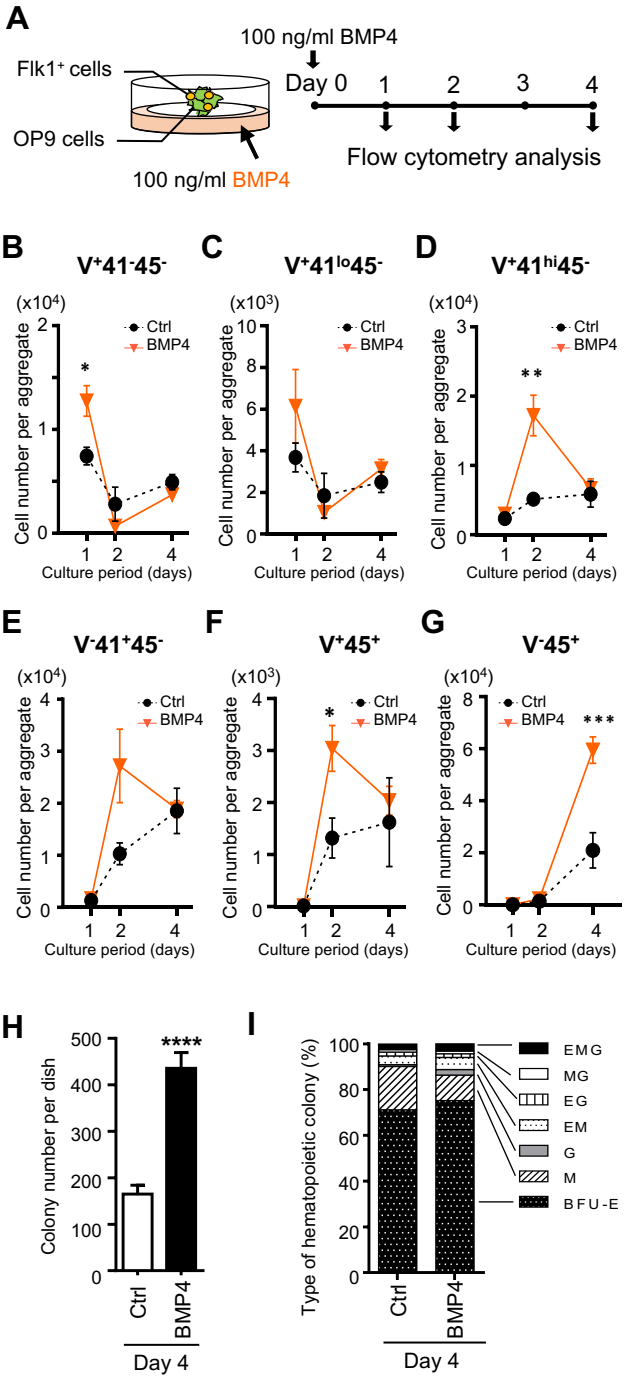
A
100 ng/ml BMP4
Flk1⁺ cells
Day 0
1
2
3
4
OP9 cells
Flow cytometry analysis
100 ng/ml BMP4
B
V⁺41⁻45⁻
C
V⁺41ˡᵒ45⁻
D
V⁺41ʰⁱ45⁻
(x10⁴)
(x10³)
Cell number per aggregate
Ctrl
BMP4
Culture period (days)
E
V⁻41⁺45⁻
F
V⁺45⁺
G
V⁻45⁺
H
Colony number per dish
Day 4
I
Type of hematopoietic colony (%)
EMG
MG
EG
EM
G
M
BFU-E

Figure 4

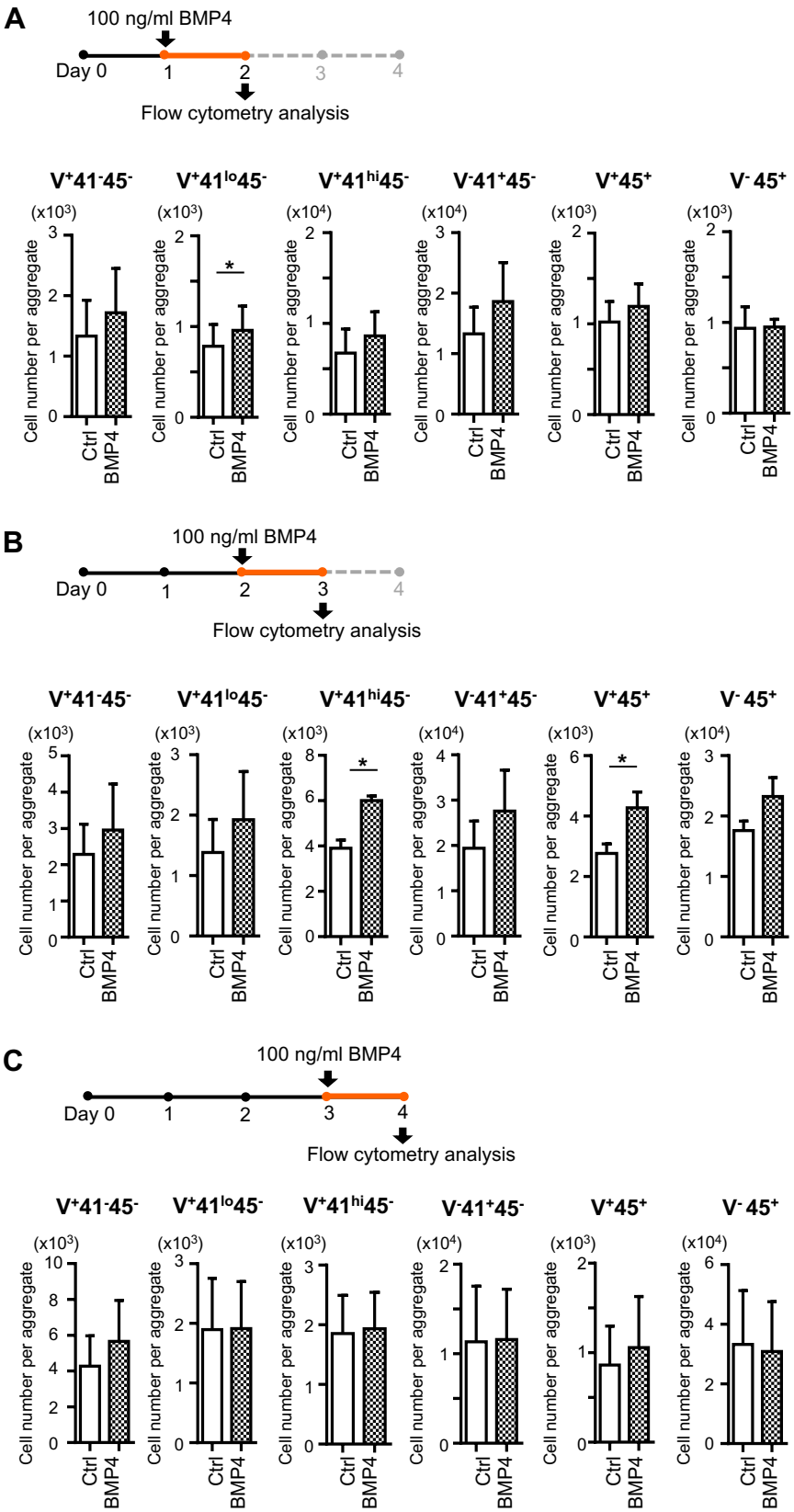
A
100 ng/ml BMP4
Day 0
1
2
3
4
Flow cytometry analysis
V+41-45-
V+41lo45-
V+41hi45-
V-41+45-
V+45+
V-45+
(x10³)
(x10⁴)
Cell number per aggregate
Ctrl
BMP4
*
B
100 ng/ml BMP4
Day 0
Flow cytometry analysis
C
100 ng/ml BMP4
Day 0
Flow cytometry analysis

Figure 5

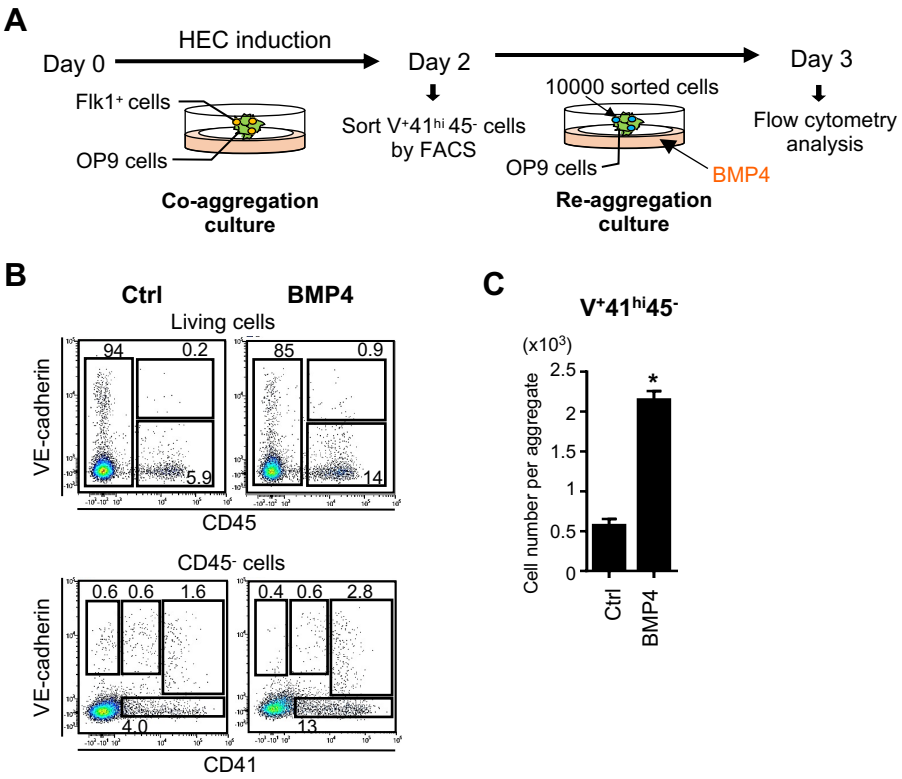
A
HEC induction
Day 0
Day 2
Day 3
Flk1+ cells
OP9 cells
Co-aggregation culture
Sort V+41hi45- cells by FACS
10000 sorted cells
OP9 cells
BMP4
Re-aggregation culture
Flow cytometry analysis
B
Ctrl
BMP4
Living cells
VE-cadherin
CD45
94
0.2
5.9
85
0.9
14
CD45- cells
VE-cadherin
CD41
0.6
0.6
1.6
4.0
0.4
0.6
2.8
13
C
V+41hi45-
(x10³)
Cell number per aggregate
2.5
2
1.5
1
0.5
0
*
Ctrl
BMP4

Figure 6

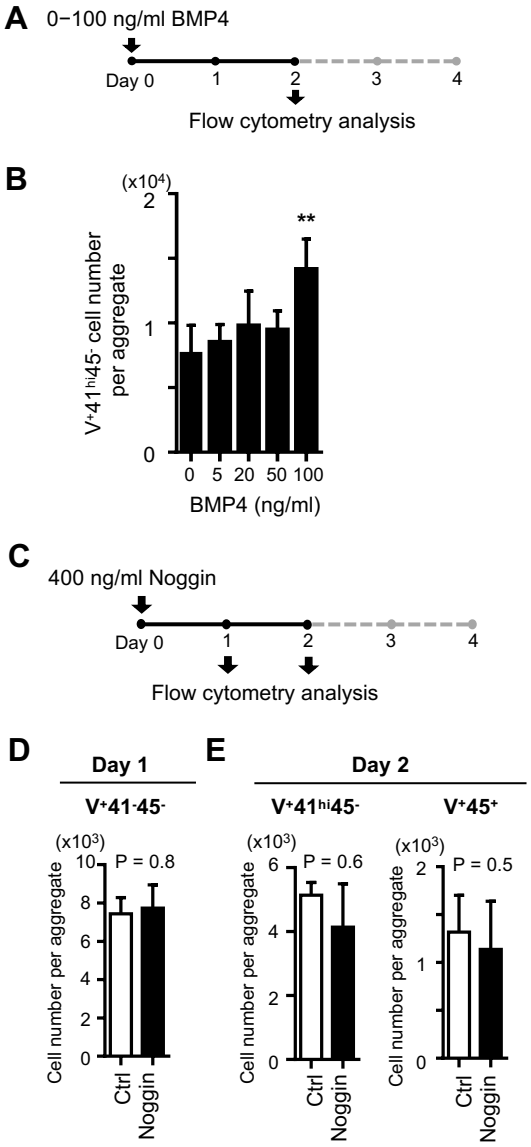
A
0−100 ng/ml BMP4
Day 0
1
2
3
4
Flow cytometry analysis
B
(x10⁴)
2
1
0
**
V⁺41ʰⁱ45⁻ cell number per aggregate
0 5 20 50 100
BMP4 (ng/ml)
C
400 ng/ml Noggin
Day 0
1
2
3
4
Flow cytometry analysis
D
Day 1
V⁺41⁻45⁻
(x10³)
10
8
6
4
2
0
P = 0.8
Cell number per aggregate
Ctrl
Noggin
E
Day 2
V⁺41ʰⁱ45⁻
V⁺45⁺
(x10³)
6
4
2
0
P = 0.6
Cell number per aggregate
Ctrl
Noggin
(x10³)
2
1
0
P = 0.5
Cell number per aggregate
Ctrl
Noggin

Supplemental Figure Legends

Supplemental Figure S1. Comparison of OP9 co-aggregation culture and OP9 monolayer co-culture

(A) Schematic diagram of ESC differentiation culture. ESCs were cultured on an OP9 cell layer for four days. Flk1$^+$ mesodermal cells were isolated by MACS. For OP9 monolayer co-culture, Flk1$^+$ cells (3×10^5 cells per culture) were seeded on an OP9 cell layer, which consisted of around 3×10^5 OP9 cells prepared in a T25 flask, and cultured in the induction medium. For OP9 co-aggregation culture, Flk1$^+$ cells (1×10^5 cells) were co-aggregated with OP9 cells (1×10^5 cells). Three aggregates were cultured on a membrane filter floating on the induction. After four days, cell aggregates were dissociated in 1 mg/ml Collagenase/Disperse™ at 37 ℃ for 40 min. The monolayer co-culture was first incubated with 0.53 mM EDTA in Hanks' balanced salt solution at 37 ℃ for 20 min and collected cells were treated with Collagenase/Disperse™ as above. Harvested cells were analyzed by flow cytometry. **(B)** Representative profiles of CD45, VE-cadherin, and CD41 expression on cultured cells. Numbers indicate the percentage of cells in the rectangular regions. Four independent experiments were performed. **(C–H)** Percentage of VE-cadherin$^+$CD41$^-$CD45$^-$ (V$^+$41$^-$45$^-$) cells (C), VE-cadherin$^+$CD41^{lo}CD45$^-$ (V$^+$41^{lo}45$^-$) cells (D), VE-cadherin$^+$CD41^{hi} CD45$^-$ (V$^+$41^{hi}45$^-$) cells (E), VE-cadherin$^-$CD41$^+$CD45$^-$ (V$^-$41$^+$45$^-$) cells (F), VE-cadherin$^+$CD45$^+$ (V$^+$45$^+$) cells (G), and VE-cadherin$^-$CD45$^+$ (V$^-$45$^+$) cells (H) in living cells. n=4 from four independent experiments. *$p < 0.05$, **$p < 0.01$ in Student's T-test. **(I–O)** Number of total cells (I) V$^+$41$^-$45$^-$ cells (J), V$^+$41^{lo}45$^-$ cells (K), V$^+$41^{hi}45$^-$ cells (L), V$^-$41$^+$45$^-$ cells (M), V$^+$45$^+$ cells (N), and V$^-$45$^+$ cells (O) per culture (monolayer co-culture) or three aggregates (co-aggregation culture). n=4 from four independent experiments. *$p < 0.05$, **$p < 0.01$, ***$p < 0.001$ in Student's T-test. **(P)** Representative profiles of Lyve1 expression on V$^+$41$^-$45$^-$ cells from monolayer co-culture, co-aggregation culture, E10.5 mouse yolk sac, or E10.5 aorta-gonad-mesonephros (AGM) region. Numbers indicate the percentage of cells in the rectangular regions. Three independent experiments were performed. **(Q)** Percentage of Lyve1$^+$ cells in V$^+$41$^-$45$^-$ endothelial cells. n=3 from three independent experiments. *$p < 0.05$, ***$p < 0.001$, ****$p < 0.0001$, in Tukey's multiple comparisons test.

Supplemental Figure S2. mRNA expression in the ESC-derived Flk1$^+$ cell culture, murine yolk sac, embryo proper, and the AGM region determined by quantitative RT-PCR

OP9 cells were aggregated with or without ESC-derived Flk1$^+$ cells and cultured for four days. The yolk sac (YS), embryo proper (EP), or AGM region were isolated from E9.5 or E10.5 mouse embryos. The embryonic tissues and ESC-derived cell-aggregates were dissociated using 1 mg/ml Collagenase/Disperse™ to obtain a single-cell suspension. RNA was extracted using RNeasy Micro Kit (QIAGEN, Venlo, Nederland) and cDNA was prepared using PrimeScript RT reagent Kit (Takara Bio, Shiga, Japan). qPCR was performed using TB Premix Ex Tag™ II and ROX Reference Dye (Takara Bio). The list of the primers (10 μM) is provided in the Supplemental Information. cDNA was amplified (one cycle of 95℃ for 30 sec; 40 cycles of 95℃ for 5 sec and 60℃ for 31 sec) using ABI7300 Fast Real-Time PCR System (Applied Biosystems, Waltham, MA, USA). The expression level of target genes was normalized to the *Gapdh* expression. **(A)** Expression of *Hoxa9*, *Hbb-bs*, and *Hbb-y* in aggregates of OP9 cells, co-aggregates of OP9 cells and Flk1$^+$ cells , E10.5 YS, and E10.5 AGM. **(B)** Expression of *Bmp4*, *Noggin*, and *Bmper* in co-aggregates of OP9 cells and Flk1$^+$ cells , E10.5 AGM, and E9.5 EP. n=3 from three independent experiments. *$p < 0.05$, ** $p < 0.01$, *** $p < 0.001$, ****$p < 0.0001$ in Dunnett's multiple comparison test vs. co-aggregates of OP9 cells and Flk1$^+$ cells.

Supplemental Figure S3. Flow cytometry analyses of cells cultured in the presence or absence of BMP4 (long-term treatment)

(A) Experimental design. ESC-derived Flk1$^+$ cells and OP9 cells were co-aggregated and cultured in the presence or absence of BMP4 (100ng/ml) for one, two, or four days. Cultured cells were analyzed for VE-cadherin, CD41, and CD45 expression by flow cytometry. **(B–D)** Representative profiles of VE-cadherin, CD41, and CD45 expression on the cells cultured for one day (B), two days (C), or four days (D). Left panels (Ctrl) show the profiles in the absence of BMP4. Right panels (BMP4) show the profiles in the presence of BMP4. Numbers indicate the percentage of cells in the rectangular regions. Four independent experiments (one and two days) or five independent experiments (four days) were performed. The nomenclature of cell populations is depicted in the panel (D). V, VE-cadherin; 41, CD41; 45, CD45.

Supplemental Figure S4. Flow cytometry analyses of cells cultured in the presence or absence of BMP4 (short-term treatment)

(A−C) Representative profiles of VE-cadherin, CD41, and CD45 expression on cultured cells. ESC-derived $Flk1^+$ cells and OP9 cells were co-aggregated and cultured. BMP4 (100ng/ml) was added on day 1 (A), day 2 (B), or day 3 (C). After a one-day treatment of BMP4, cells were analyzed for VE-cadherin, CD41, and CD45 expression by flow cytometry. Left panels (Ctrl) show the profiles in the absence of BMP4. Right panels (BMP4) show the profiles in the presence of BMP4. Numbers indicate the percentage of cells in the rectangular regions. Three independent experiments were performed. The nomenclature of cell populations is depicted in panel (C). V, VE-cadherin; 41, CD41; 45, CD45.

Supplemental Figure S5. Inhibition of BMP4-induced increase of $V^+41^{hi}45^-$ cells and V^+45^+ cells by Noggin and ALK2/3 inhibitor

(A) Experimental design. $Flk1^+$ cells and OP9 cells were co-aggregated and cultured in the presence or absence of BMP4 (100ng/ml), Noggin (400 ng/ml), and LDN-193189 (0.01μM) (MedChemExpress, Monmouth Junction, NJ, USA) for two days. Cultured cells were analyzed for VE-cadherin, CD41, and CD45 expression by flow cytometry. **(B, C)** The number of VE-cadherin$^+$CD41^{hi}CD45$^-$ ($V^+41^{hi}45^-$) and VE-cadherin$^+$CD45$^+$ (V^+45^+) cells per aggregate. n=3 from three independent experiments. *$p < 0.05$ in Dunnett's multiple comparison vs. control.

Supplemental Figure S1

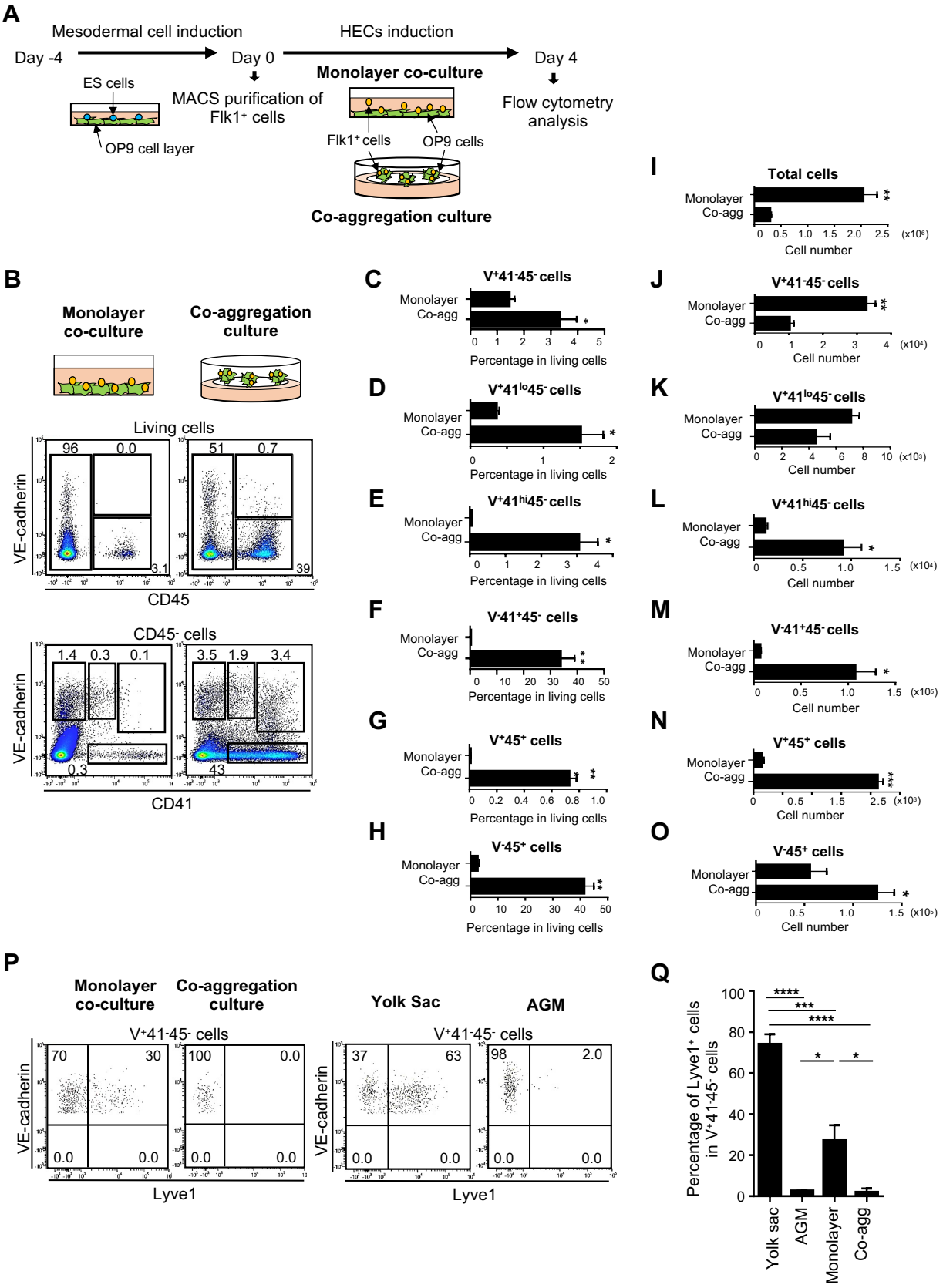

Supplemental Figure S2

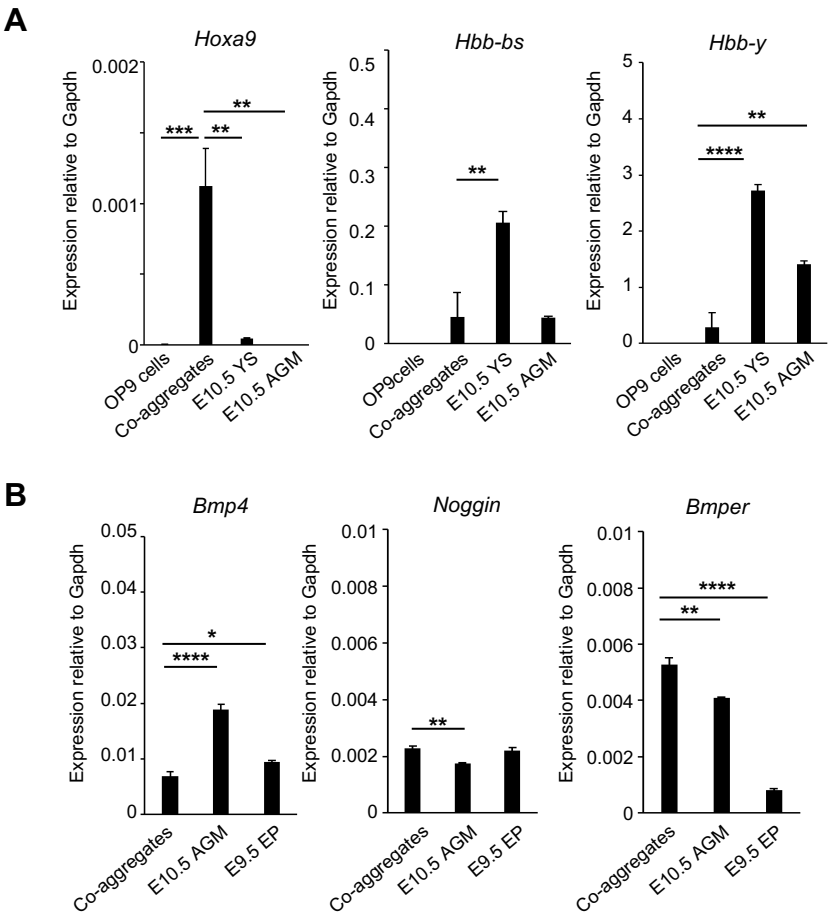

Supplemental Figure S3

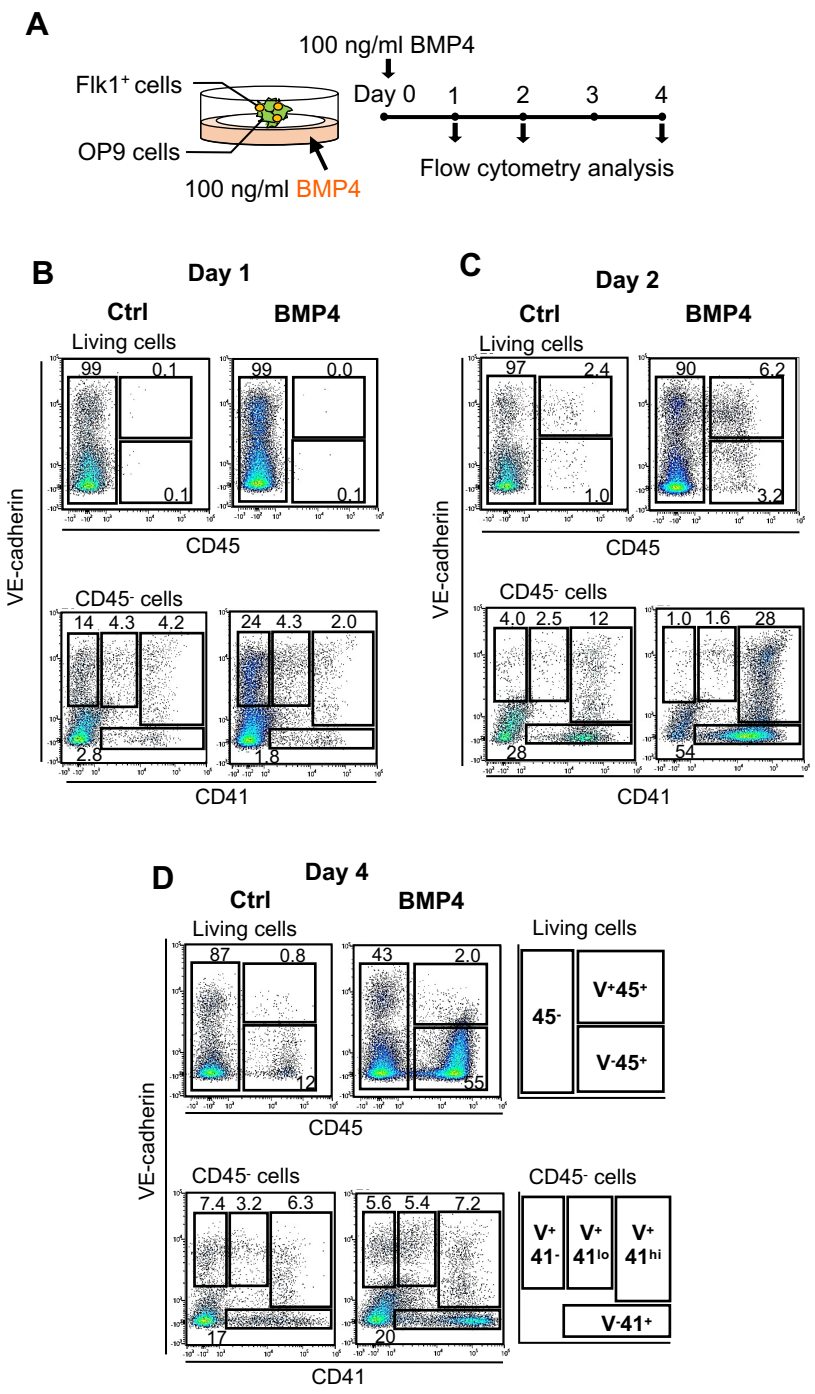

Supplemental Figure S4

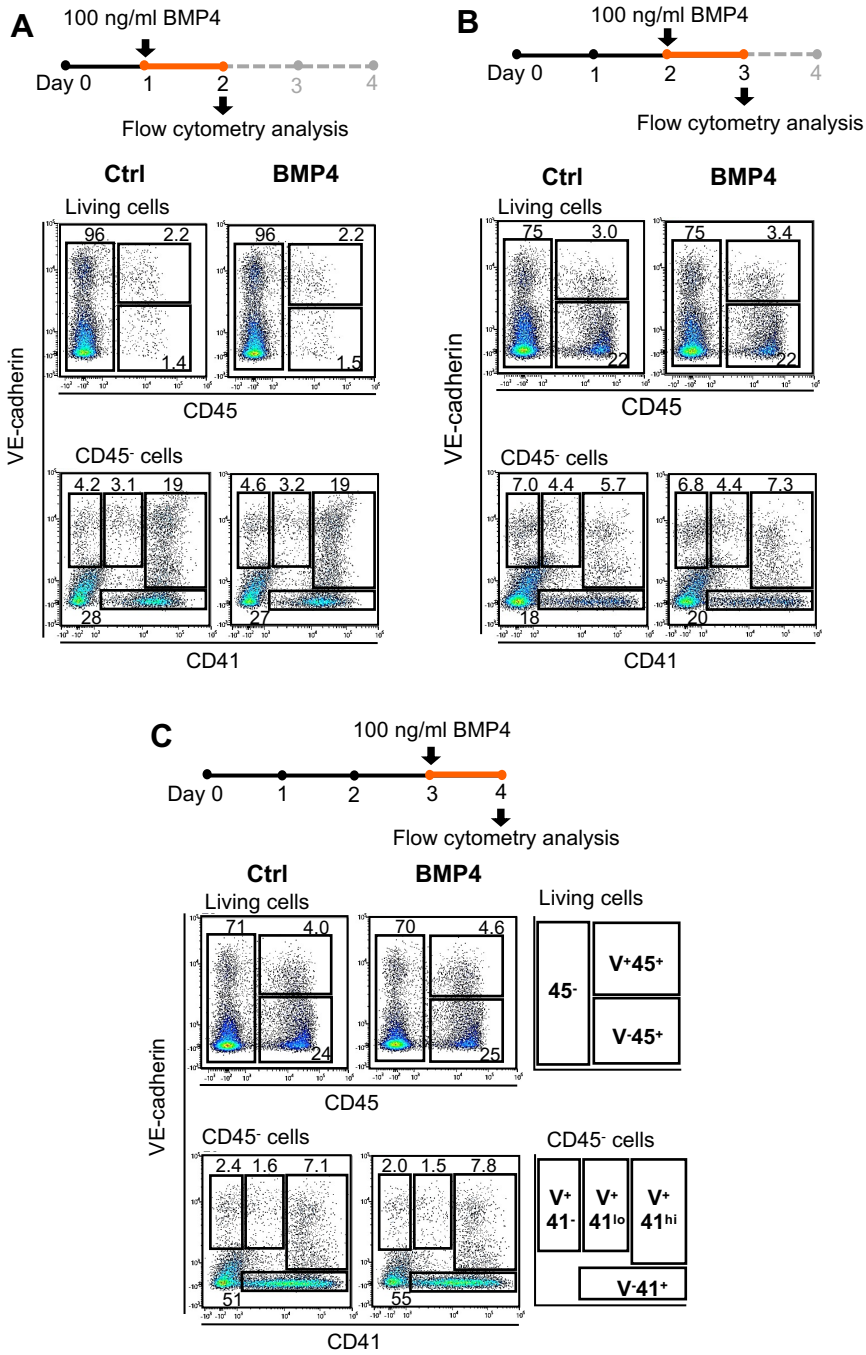

Supplemental Figure S5

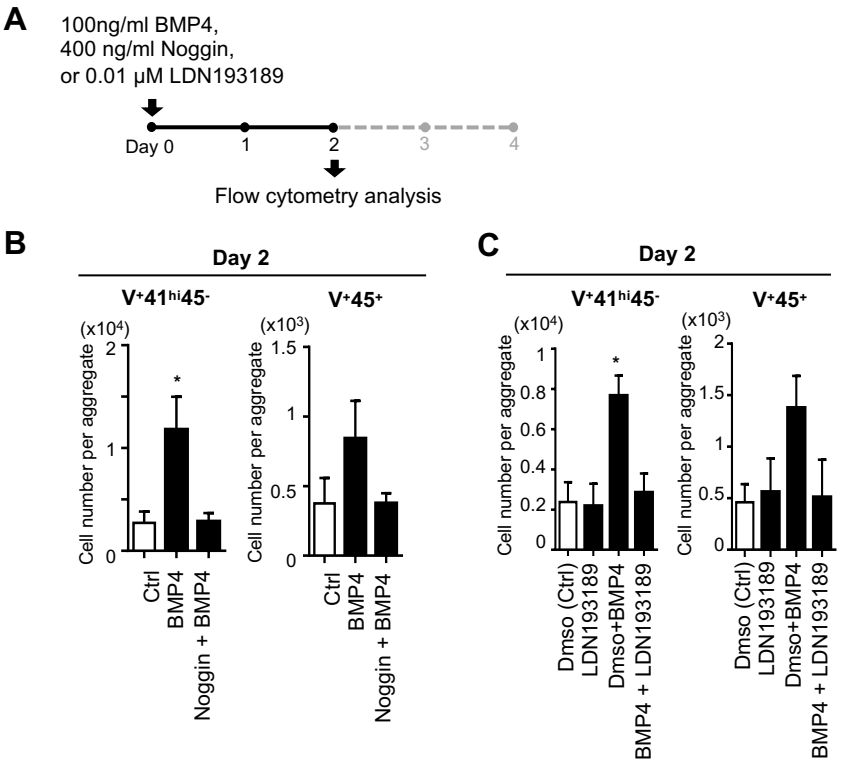

Supplemental Table S1: Monoclonal antibodies used in this study

Experiment	Target	Reactivity	Clone	Conjugate	Source
Flk1^{+} mesodermal cell sorting	**Flk1**	mouse	Avas12	Phycoerythrin (PE)	BioLegend, San Diego, CA, USA
Flow cytometry analysis and cell sorting	**VE-cadherin**	mouse	BV13	Brilliant Violet 421™ (BV421)	BioLegend
	CD31	mouse	390	Fluorescein Isothiocyanate (FITC)	BioLegend
	CD41	mouse	MWReg30	PE	BioLegend
	CD45	mouse	30-F11	Allophycocyanin (APC)	eBioscience™, Thermo Fisher Scientific
Flow cytometry analysis of hematopoietic cells	**CD71**	mouse	C2	FITC	BD, Franklin Lakes, NJ, USA
	TER-119	mouse	TER-119	PE	eBioscience
	Gr-1	mouse	RB6-8C5	Peridinin Chlorophyll Protein (PerCP)	BioLegend
	CD11b	mouse/human	M1/70	APC	BioLegend
	CD4	mouse	GK1.5	Alexa Fluor 700 (AF700)	eBioscience
	CD8a	mouse	53-6.7	APC	BioLegend
Flow cytometry analysis of the expression of Lyve1	**Lyve1**	mouse	ALY7	eFluor 660	eBioscience
	VE-cadherin	mouse	BV13	BV421	BioLegend
	CD31	mouse	390	FITC	BioLegend
	CD41	mouse	MWReg30	PE	BioLegend
	CD45	mouse	30-F11	AF700	eBioscience
Dead cell staining	**Dead cells**	-	-	Propidium Iodide (PI)	Merk

Supplemental Table S2: Primers used in this study

Target gene	Reactivity	Arrangement (5'→3')		Annealing temperature (°C)	Amplicon length (bp)	Reference
Gapdh	mouse	Forward	ATGGTGAAGGTCGGTGTGAA	52	108	Maud F. et al., Int. J. Dev. Biol. 54: 1067-1074 (2010), doi: 10.1387/ijdb.103104mf
		Reverse	AATGAAGGGGTCGTTGATGG			
Hoxa9	mouse	Forward	ACAATGCCGAGAATGAGAGC	52	129	Kim YJ. et al., PNAS, 108 (18) 7391-7396 (2011), doi: 10.1073/pnas.1018279108
		Reverse	GTTCCAGCGTCTGGTGTTTT			
Hbb-y	mouse	Forward	TGGCCTGTGGAGTAAGGTCAA	54	120	Primer Bank, https://pga.mgh.harvard.edu/primerbank/, ID: 6680177a1
		Reverse	GAAGCAGAGGACAAGTTCCCA			
Hbb-bs	mouse	Forward	GTGAACGCCGATGAAGTTG	51	108	Yang L., Protein & Cell, volume 9, pages 814–819 (2018), doi: 10.1007/s13238-018-0568-x
		Reverse	AGCAGAGGCAGAGGATAGGTC			
BMP4	mouse	Forward	GAGGAGTTTCCATCACGAAGA	51	122	McGarvey A. C., JEM., 214(12):3731-3751 (2017), doi: 10.1084/jem.20162012
		Reverse	GCTCTGCCGAGGAGATCA			
Noggin	mouse	Forward	GCCAGCACTATCTACACATCC	52	114	Primer Bank, https://pga.mgh.harvard.edu/primerbank/, ID: 7110675a1
		Reverse	GCGTCTCGTTCAGATCCTTCTC			
BMPER	mouse	Forward	TGTGCAAGTTCGGTAGCAAG	52	60	McGarvey A. C., JEM., 214(12):3731-3751 (2017), doi: 10.1084/jem.20162012
		Reverse	TGCAGTTGACTGAGGACCAC			